CRREL
REPORT 86-1

US Army Corps of Engineers
Cold Regions Research & Engineering Laboratory

Model studies of ice interaction with the U.S. Army Ribbon Bridge

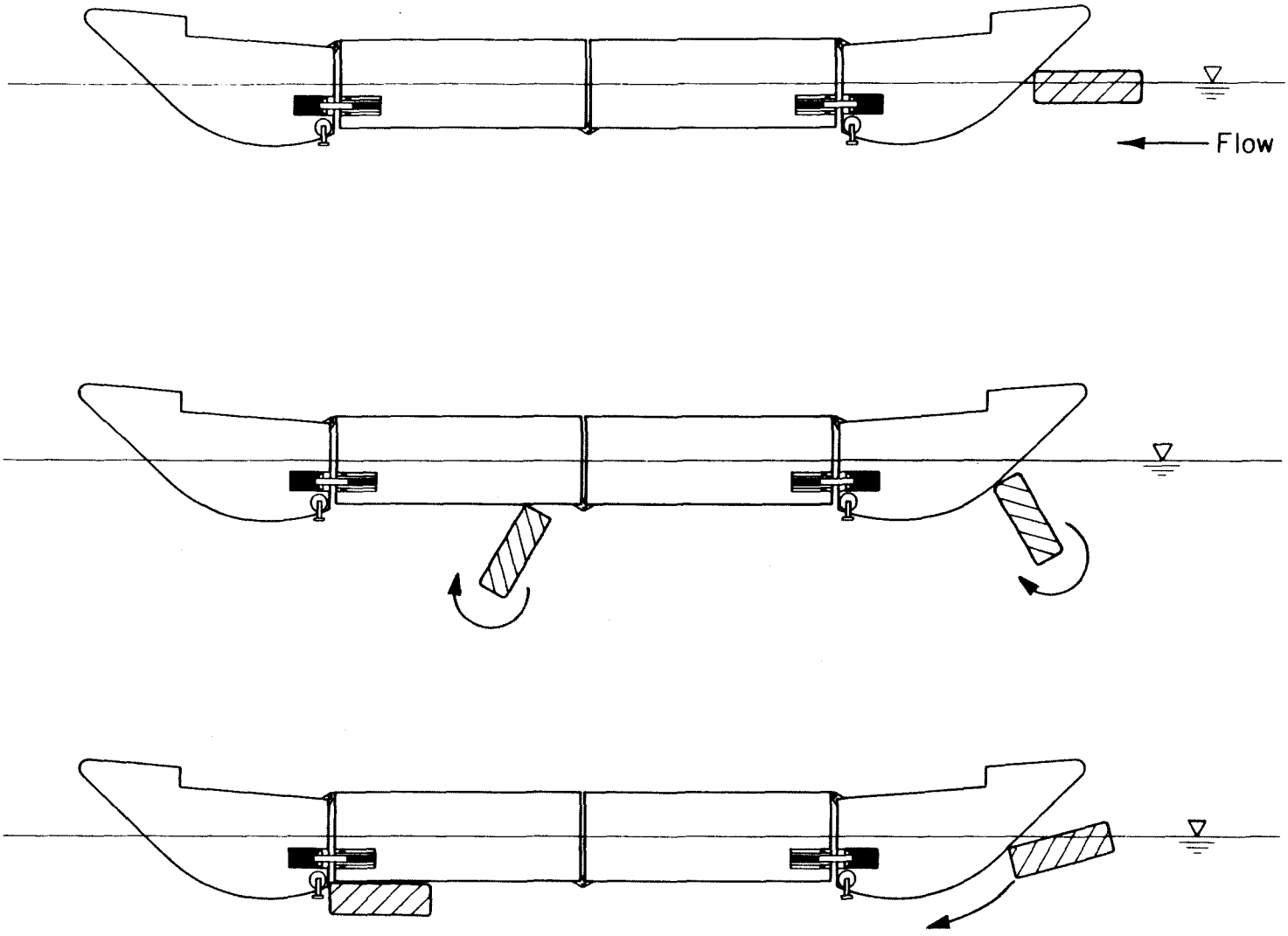

CRREL Report 86-1

April 1986

Model studies of ice interaction with the U.S. Army Ribbon Bridge

Barry A. Coutermarsh

Prepared for
OFFICE OF THE CHIEF OF ENGINEERS

Unclassified

SECURITY CLASSIFICATION OF THIS PAGE (When Data Entered)

REPORT DOCUMENTATION PAGE

READ INSTRUCTIONS BEFORE COMPLETING FORM

1. REPORT NUMBER: CRREL Report 86-1

2. GOVT ACCESSION NO.:

RECIPIENT'S CATALOG NUMBER:

4. TITLE (and Subtitle): MODEL STUDIES OF ICE INTERACTION WITH THE U.S. ARMY RIBBON BRIDGE

TYPE OF REPORT & PERIOD COVERED:

6. PERFORMING ORG. REPORT NUMBER:

7. AUTHOR(s): Barry A. Coutermarsh

8. CONTRACT OR GRANT NUMBER(s):

9. PERFORMING ORGANIZATION NAME AND ADDRESS: U.S. Army Cold Regions Research and Engineering Laboratory, Hanover, New Hampshire 03755-1290

10. PROGRAM ELEMENT, PROJECT, TASK AREA & WORK UNIT NUMBERS: DA Project 4A762730AT42, Task A, Work Unit 008

11. CONTROLLING OFFICE NAME AND ADDRESS: Office of the Chief of Engineers, Washington, D.C. 20314-1000

12. REPORT DATE: April 1986

13. NUMBER OF PAGES: 22

14. MONITORING AGENCY NAME & ADDRESS (if different from Controlling Office):

15. SECURITY CLASS. (of this report): Unclassified

15a. DECLASSIFICATION DOWNGRADING SCHEDULE:

16. DISTRIBUTION STATEMENT (of this Report)

Approved for public release; distribution is unlimited.

17. DISTRIBUTION STATEMENT (of the abstract entered in Block 20, if different from Report)

18. SUPPLEMENTARY NOTES

19. KEY WORDS (Continue on reverse side if necessary and identify by block number)

Bridges
Cold regions
Military bridges
Military operations
Ribbon Bridge

20. ABSTRACT (Continue on reverse side if necessary and identify by block number)

The performance of the U.S. Army's floating Ribbon Bridge in an ice-filled waterway is investigated in a model study. Conditions when ice-blocks could be expected to jam behind the bridge are outlined using available instability theories. It is shown that current theories do not accurately describe block instability throughout the range of expected block thicknesses. Bridge deployment doctrine is outlined as it relates to the winter environment. Ice forces on the bridge are discussed along with ways to minimize the chance of ice build-up behind the bridge.

DD FORM 1 JAN 73 1473 EDITION OF 1 NOV 65 IS OBSOLETE

Unclassified

SECURITY CLASSIFICATION OF THIS PAGE (When Data Entered)

PREFACE

This report was prepared by Barry A. Coutermarsh, Research Civil Engineer, of the Applied Research Branch, Experimental Engineering Division, U.S. Army Cold Regions Research and Engineering Laboratory. This study was funded under DA project 4A762730AT42, *Design, Construction and Operations Technology for Cold Regions*; Task CS, *Combat Support*; Work Unit 001, *Cold Weather Bridging*.

The author thanks Steven Daly of CRREL for his patient discussions of instability theory and technical review of this report. Paul Richmond of CRREL also technically reviewed this report.

The operational practices and procedures discussed in this report do not necessarily represent approved doctrine or support for deployment of the Ribbon Bridge in an ice-filled waterway. Nor should it be implied that the test program described herein represents an extensive effort to establish the complete capability or reaction of the Ribbon Bridge to cold weather operations.

CONTENTS

ILLUSTRATIONS

Figure

TABLE

Table

CONVERSION FACTORS: U.S. CUSTOMARY TO METRIC (SI) UNITS OF MEASUREMENT

These conversion factors include all the significant digits given in the conversion tables in the ASTM *Metric Practice Guide* (E 380), which has been approved for use by the Department of Defense. Converted values should be rounded to have the same precision as the original (see E 380).

Multiply	By	To obtain
inch	25.4	millimetre
foot	0.3048	metre
pound (mass)	0.4535924	kilogram
ton	907.1847	kilogram
gallon per minute	0.0000630902	cubic metre per second
foot per second	0.3048	metre per second
pound per square foot	4.882428	kilogram per square metre

MODEL STUDIES OF ICE INTERACTION WITH THE U.S. ARMY RIBBON BRIDGE

Barry A. Coutermarsh

INTRODUCTION

River crossings

Mobility is the key to rapid response on the battlefield of the future. ALBE (AirLand Battlefield Environment) doctrine dictates that ground-based forces must be able to move freely and quickly to be an effective strike force that is less exposed to retaliation. A river crossing is a relatively vulnerable operation that could greatly reduce the flexibility and momentum of forces on the move. A winter environment added to the normal conditions associated with river crossings can make an otherwise routine exercise nearly impossible. The field commander needs to know the conditions under which a winter crossing can be attempted and the problems to be expected from such an operation to accurately assess the probability of success.

This paper will delimit some of the conditions associated with the use of the U.S. Army Ribbon Bridge in a winter river crossing. The propensity of the bridge to initiate an ice jam is evaluated in a model study and the conditions under which jamming can be expected are outlined. The forces expected during a jam are discussed along with suggestions for doctrine changes to minimize the effect of ice on a winter river crossing.

Ribbon Bridge

The Ribbon Bridge is one of the primary floating tactical bridges in the Army inventory. It is a modular bridge, consisting of individual foldable aluminum sections or bays (Fig. 1) that are transported to the crossing site on modified M812, 5-ton trucks. The truck is modified with a special cradle to hold the bridge bay, along with a hydraulically operated boom to assist in loading and unloading. Each interior bay is reinforced aluminum, and has two roadway pontons and two bow pontons. When the bay is launched, these pontons unfold to form a bridge bay (Fig. 2) that is approximately 22 ft long by 26.7 ft wide by 2.5 ft thick, weighing about 12,000 lb. Ramp bays are similar in construction, with unfolded dimensions of 18.3 ft long by 26.7 ft wide by 2.5 ft thick at the offshore end and 1.25 ft thick at the shore end. A 7-ft-long adjustable ramp is hinged to the roadway portion of the bay to allow vehicles to get on and off the bridge. The ramp bay weighs approximately 11,750 lb. A completed bridge consists of interior bays joined together with ramp bays at each end. The various bays are held together by "dogbone" connectors (Fig. 1). These connectors allow movement between bays while maintaining the overall integrity of the bridge. Bay sections are also used as rafts

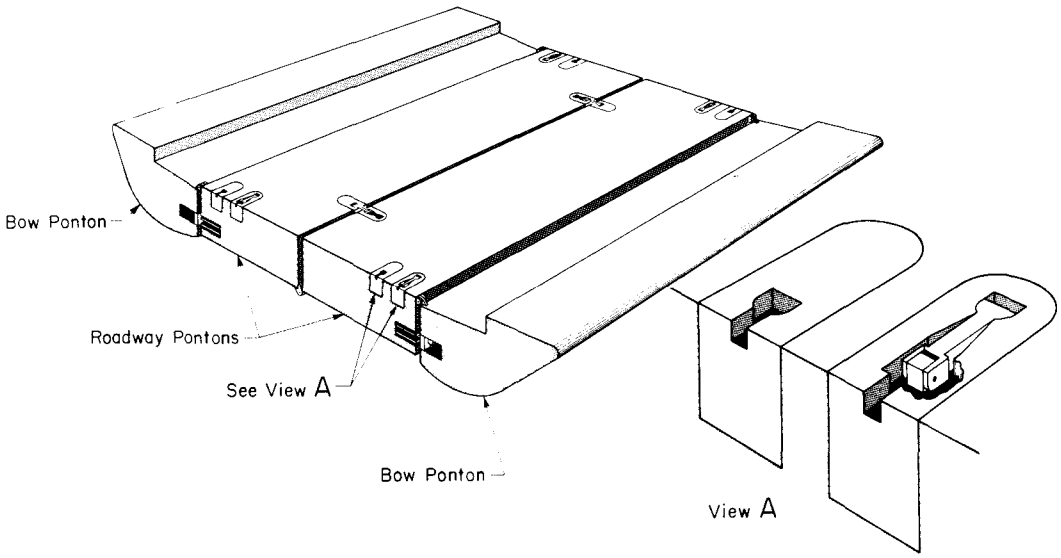

Figure 1. Ribbon Bridge bay with dogbone detail.

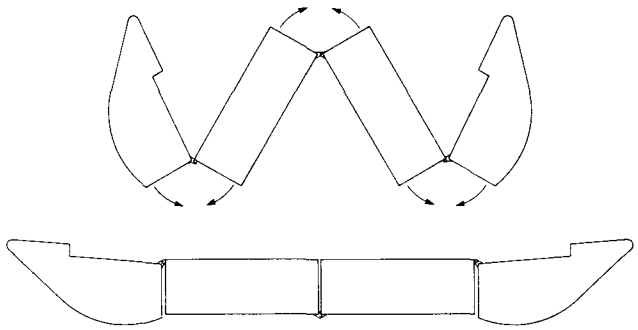

Figure 2. View of bridge bay unfolding sequence (top) and bay in unfolded position.

Figure 3. Profile view of bridge interior bay.

with the addition of a propulsive source. Stubstad et al. (1984) look at the problems associated with one propulsive source, the U.S. Combat Support Boat (USCS BMK I), or Bridge Erection Boat (BEB), when used with ice present in the waterway.

Figure 3 shows a profile section through an unfolded interior bay. When bridging a waterway, the sloped faces of the bow pontons are the upstream and downstream sides of the bridge. The upstream face will obviously bear the brunt of any impact from floating ice, and its shape helps determine if ice will jam against the bridge or pass beneath it. The first step in the investigation was to ascertain ice floe stability characteristics against a model of the ribbon bridge under several draft configurations.

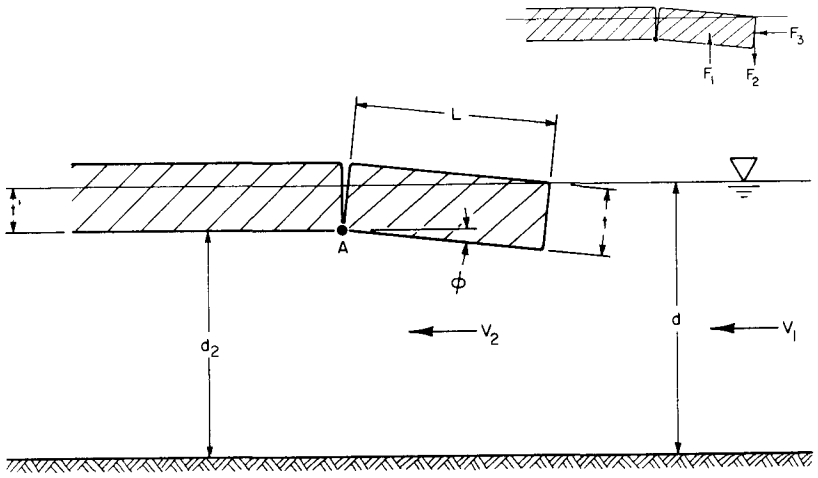

Figure 4. Physical description of block and obstruction. The insert shows the buoyancy force F_1*, the underturning force associated with the reduction in water elevation because of the increase in velocity head* F_2 *and the hydrodynamic force on the upstream face of the block* F_3.

BACKGROUND

The question of ice floe stability against a stationary object has been investigated in several previous studies, of which three are described below. These investigations have centered around a force and moment analysis to determine when a floe would reach its instability condition based on a critical Froude number, i.e., the Froude number based on the upstream flow velocity and the depth or floe thickness where the floe would become unstable, sink and pass beneath the obstruction. Figure 4 shows the physical details of the floe and a vertical obstruction along with the relevant forces associated with the problem.

Pariset and Hausser (1961) presented an analysis with the conclusion that an ice block becomes unstable when its upstream top edge submerges (the "no-spill" condition) and by assuming vertical sinking; they arrived at the following expression for instability:

$$\frac{V_1}{\sqrt{2gd}} = \varkappa \sqrt{(1-\varrho'/\varrho)(t/d)}\,[1-(t/d)] \tag{1}$$

where V_1 = fluid velocity upstream from the block
g = gravitational acceleration
t = block thickness
ϱ' = block density
ϱ = water density
d = depth of the fluid just upstream of the block.

The coefficient $\varkappa$ is an empirical parameter and was included to allow for the fact that most blocks submerge by underturning at a generally lower velocity than predicted by eq 1. A later paper by Pariset et al. (1966) uses eq 1 without $\varkappa$ included.

Ashton (1974) developed an expression for block instability using a Froude number based upon block thickness rather than flow depth, and showed that a moment analysis of the problem yielded good results without use of an empirical parameter. Ashton derived the following expression, invoking the no-spill condition as the point at which the block becomes unstable:

$$\frac{V_1}{\sqrt{gt(1-\varrho'/\varrho)}} = \frac{2(1-t/d)}{\sqrt{5-3(1-t/d)^2}}. \tag{2}$$

Daly (1984) noted that none of the previous analyses could explain the accumulated experimental data over the entire range of independent variables. He also felt that the no-spill condition had no theoretical support and confused the analysis. His analysis separates the phenomenon into two cases, $t'/d \ll 1$ (deep water case) and $t'/d \approx 1$ (shallow water case), where t' is the hydrostatic equilibrium depth that the flow is at when it arrives at the obstruction or

$$t' = (\varrho'/\varrho)t. \tag{3}$$

Daly determined the value of t'/d that separates the two cases by examining data from previous studies by Uzuner and Kennedy (1972), Ashton (1974) and Larsen (1975). Taking moments about point A (see Fig. 4), Daly arrived at the following equation for the block at equilibrium

$$\varrho g\left(\frac{V_2^2}{2g} - \frac{V_1^2}{2g}\right)\frac{L^2}{2} - \varrho g\,\frac{L^3}{3}\tan\phi - \varrho g\,\frac{V_1^2}{4gd}\left(\frac{t'^3}{[1-(t'/d)]^2}\right) = 0 \tag{4}$$

where V_2 = velocity beneath the block
L = block length
ϕ = angle of the block's rotation about point A.

The first term is the underturning moment due to the reduction in water elevation caused by the increase in the velocity head. The second term is the approximate restoring moment due to the buoyancy of the block as it submerges (good for small values of ϕ), and the third term is the moment due to the hydrodynamic force of the water on the upstream face of the block, assumed to act halfway between the water surface and the submerged upstream corner of the block. Using assumptions about block instability and continuity, Daly arrives at the following expression for the block Froude number at instability

$$F_b = \frac{V_1}{\sqrt{gt}} = \frac{(4/3)^{1/2}(1-t'/d)\beta}{[1-(1-t'/d)^2-(t/d)(t/L)^2(\varrho'/\varrho)^3]^{1/2}} \tag{5}$$

where β is an empirical parameter found by fitting the above equation to the data. Daly derived his "deep water" instability equation by assuming that the block becomes unstable due to periodic forcing around the natural frequency of the block, which he surmised as being:

$$f_n = \sqrt{g/t'[1+(t/L)^2]}. \tag{6}$$

He then writes the periodic forcing in the form of a Strouhal type representation as

$$\frac{f_n t}{V_1} = C \tag{7}$$

where C is a constant. The deep water instability Froude number is then

$$\frac{V_1}{\sqrt{gt}} = \frac{C^{-1}}{\sqrt{\varrho'/\varrho[1+(t/L)^2]}} \tag{8}$$

and C is found to be ≈ 2.08 from inspection of the data.

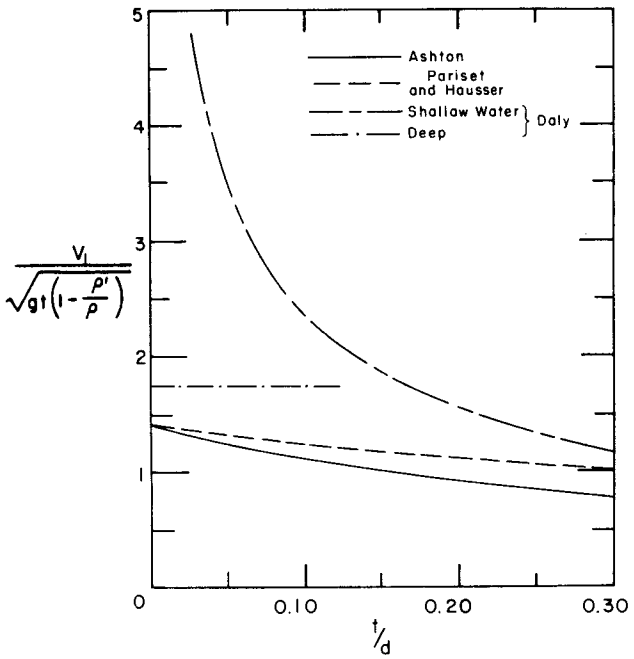

Figure 5. Four theoretical instability curves.

The equations of Pariset and Hausser and Daly are slightly rearranged to make their form the same as Ashton's, i.e., the Froude number in the form

$$\frac{V_1}{gt[1-(\varrho'/\varrho)]}\,.$$

The flow instability curves are plotted in Figure 5.

These expressions are germane to the problem of ice floe stability against the ribbon bridge; Daly's equation must be modified slightly to take into account the condition of a sloped face on the obstruction. Figure 6 shows the physical situation present when a block encounters the 45° sloped face of the bridge ponton. The obvious change in the force analysis

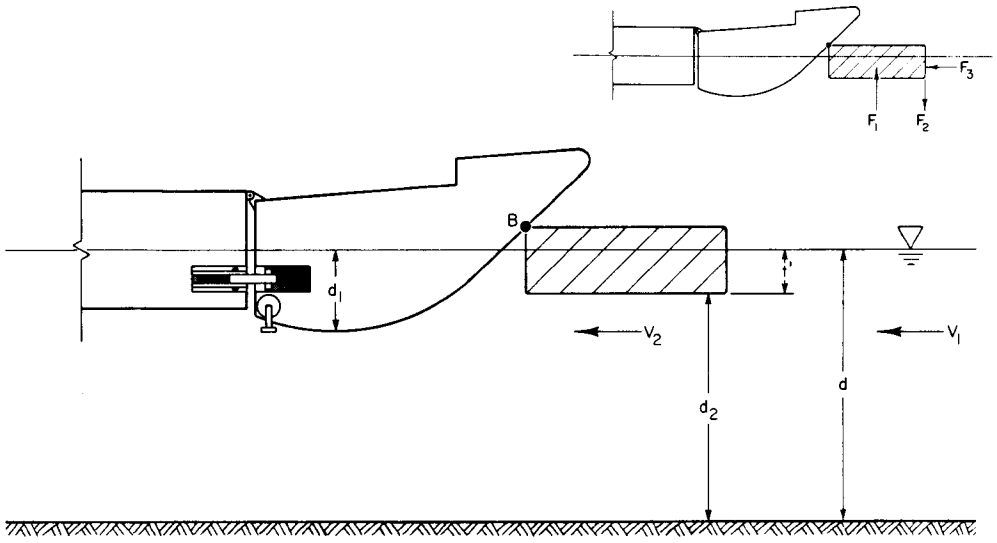

Figure 6. Physical situation when a block encounters the sloped face of the Ribbon Bridge bow ponton. F_1, F_2 *and* F_3 *are as in Figure 4.*

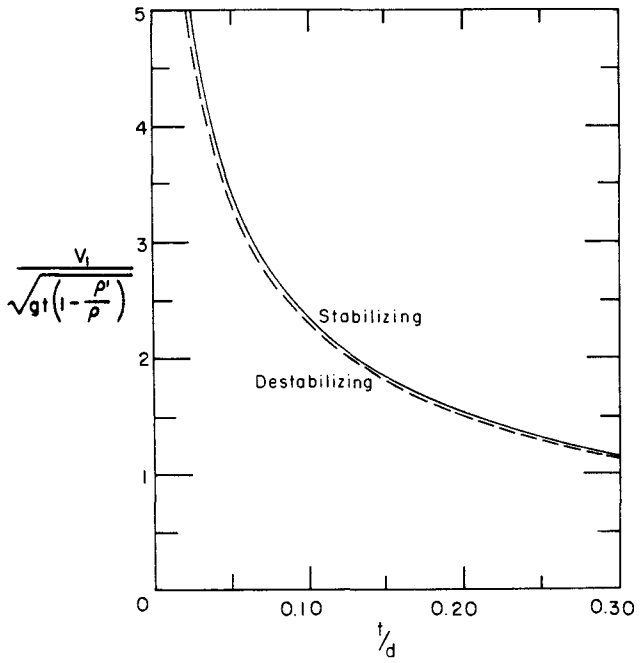

Figure 7. Daly's shallow water curve for instability, with the hydrodynamic force (F_3 in Fig. 6) as a stabilizing force (top curve) and destabilizing force (bottom curve).

is that the downstream upper corner is now the point of rotation of the block. This causes the hydrodynamic force on the upstream face of the block to be a destabilizing rather than a stabilizing force. Taking the third term in eq 4 and changing its sign to reflect this gives us the expression for the Froude number of the block at instability as:

$$F_b = \frac{V_i}{gt(1-\varrho'/\varrho)} = \frac{(4/3)^{1/2}\,(1-t'/d)\beta}{[1-(1-t'/d)^2+(t/d)(t/L)^2(\varrho'/\varrho)^3]^{1/2}}\;\frac{1}{1-\varrho/\varrho}\,. \tag{9}$$

The effect this change has on the location of the theoretical instability curve is minor, pointing out that the hydrodynamic force is not a major consideration in underturning. Figure 7 is a graph of the theoretical curves for block instability using the hydrodynamic force as a stabilizing and destabilizing force. As can be seen, there is very little difference in the curves.

MATERIALS AND METHODS

Test facility

The model study was undertaken in CRREL's warm flume, which has cross-sectional dimensions of 3 by 3 ft, a total length of 24 ft and a variable speed pumping capacity of 0 to 4800 gal./min. To simulate different water depths, a moveable plywood "river bottom" was installed in the flume. A $^1/_{20}$th scale model of an interior Ribbon Bridge section constructed of wood was suspended in the water on adjustable supports to allow for different displacement positions (Fig. 8). Ice was simulated by white polyethylene cut into four different block sizes, as shown in Table 1, with a specific gravity of approximately 0.92, comparing well with the 0.91 specific gravity of ice.

Procedure

A typical test was run as follows:

1. The bridge displacement was set at the desired depth.
2. The river bottom was set to produce the desired water depth.
3. The velocity was initially set to where all blocks would come to rest against the model.

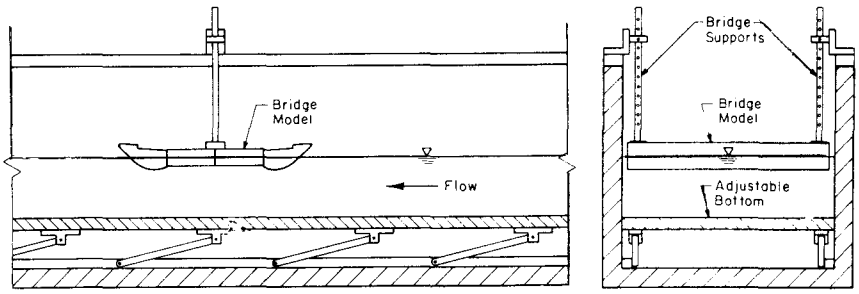

a. Cross section. *b. Side view.*

Figure 8. CRREL's warm flume.

Table 1. Dimensions of simulated ice blocks.

Block	*Size (in.)*	*Thickness/length (t/L) ratio*
1	1.5× 1.5×0.25	0.1667
2	2.0× 2.0×0.25	0.1250
3	3.875×3.875×0.25	0.0645
4	2.875×2.875×0.75	0.2609

4. The four sizes of blocks were released individually, upstream from the bridge, and allowed to jam with water velocity, bridge displacement and water depth recorded.
5. The water velocity was adjusted upwards in approximately 0.07-ft/s increments.
6. The blocks were again released individually with block response recorded along with new water velocity. Other parameters were held constant.
7. Steps 5 and 6 were repeated until all blocks passed beneath the model.
8. Either (or both) bridge displacement and water depth was changed and the test runs repeated.

RESULTS

Figure 9 is a plot of Froude number versus block thickness for the experimental data where the blocks underturn and pass beneath the model bridge, along with the previously discussed instability curves. The scatter of the points is representative of this underturning phenomenon and is found in all the previous investigations. Note also that the data were collected primarily in what Daly characterized as the deep water region ($t'/d \ll 0.1$). It will be shown later this is where existing theories poorly explain block stability, yet this is the region where the bridge is most likely to be used. It is evident the thicker blocks underturn at generally lower Froude numbers than what Daly's theory predicts. The trend is most pronounced at values of $t'/d < 0.2$, while the results obtained using the thinner blocks (1–3) agree reasonably well with theory.

The curves of Ashton and Pariset and Hausser both underestimate the point at which the thinner blocks become unstable. They both, however, describe the thicker blocks' instability, with Ashton's slightly better here. Daly's description of instability in deep water does not explain the data from this experiment for either block thickness.

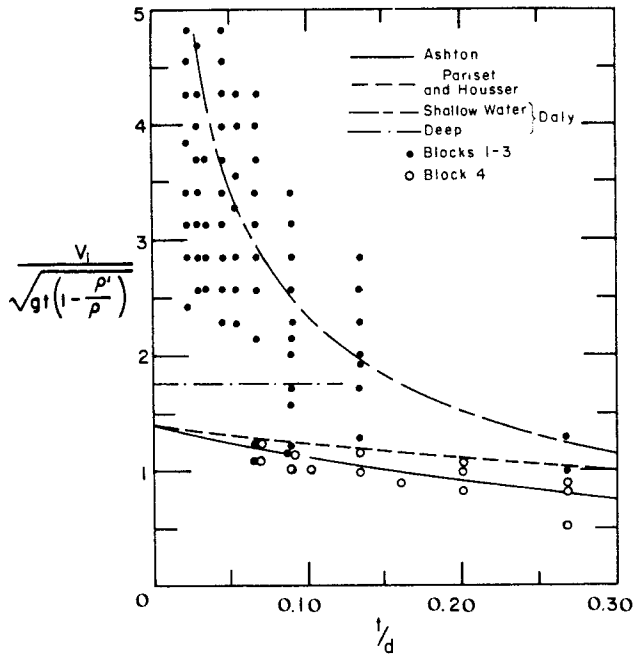

Figure 9. Four instability curves superimposed onto the underturning data for all blocks used in the experiments. The number of data points shown for blocks 1-3 is misleading. Different t/L *ratios usually made no difference in underturning events and consequently many of the points shown are three exact replicates for different* t/L ratios.

Three bridge displacements were used in the model study to represent conditions of no load (0.34 in.), a military load (MLC 70) of 70 tons (1.5 in.) and the maximum probable displacement, similar to a Heavy Equipment Transport (HET) with a MLC 70 load on it (2.0 in.). Figure 10 shows the effect bridge displacement has on block stability. For clarity, only data for blocks 1-3 are shown. There is a trend of decreasing stability with decreasing displacement evident in the figures.

Adding data for blocks jamming behind the bridge gives us the ability to define regions where jamming will or will not happen.

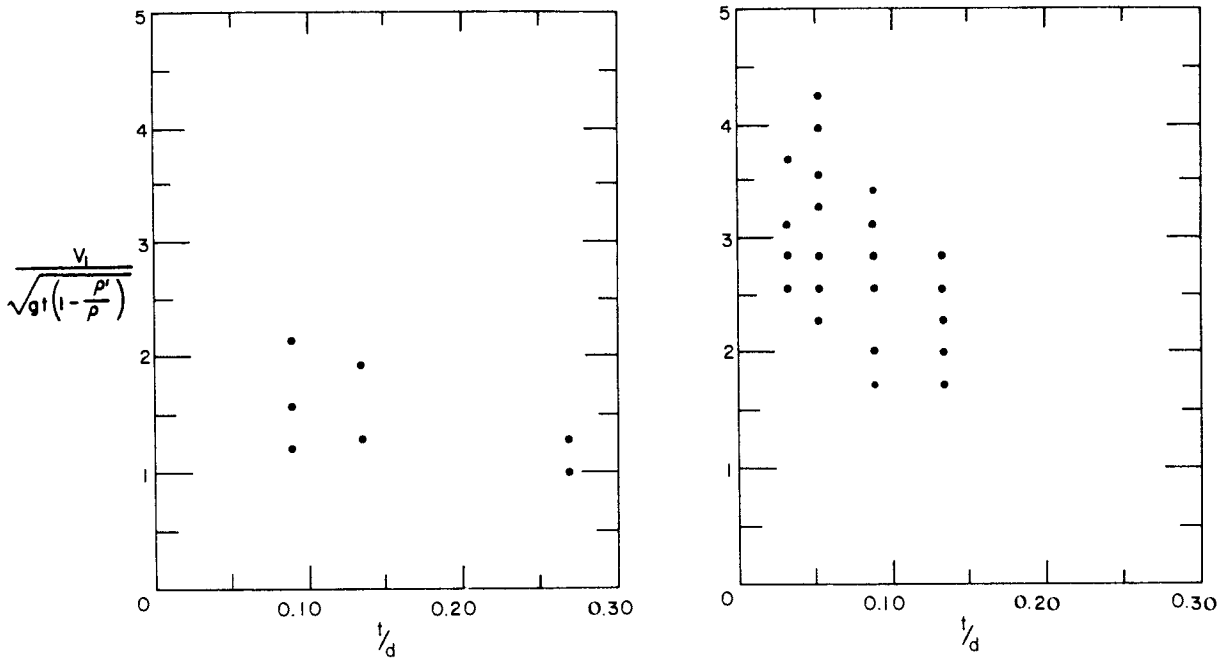

a. Displacement at 0.34 in.

b. Displacement at 1.5 in.

Figure 10. Effect of bridge displacement on block stability.

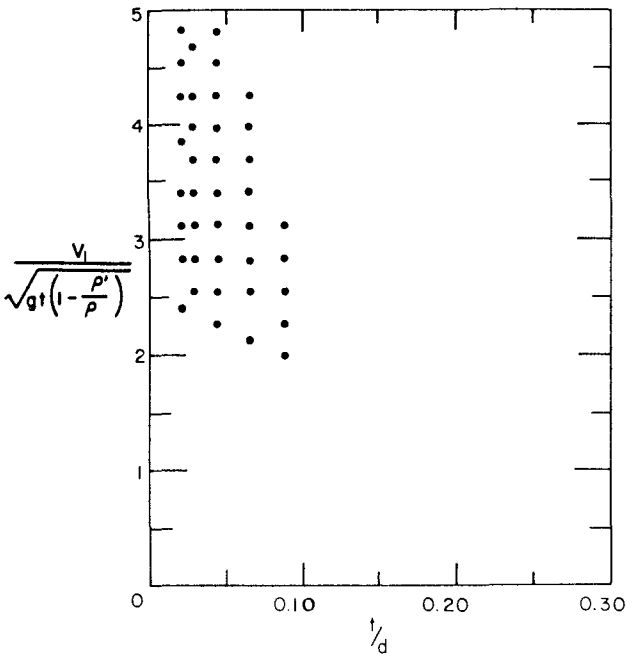

c. Displacement at 2.0 in.

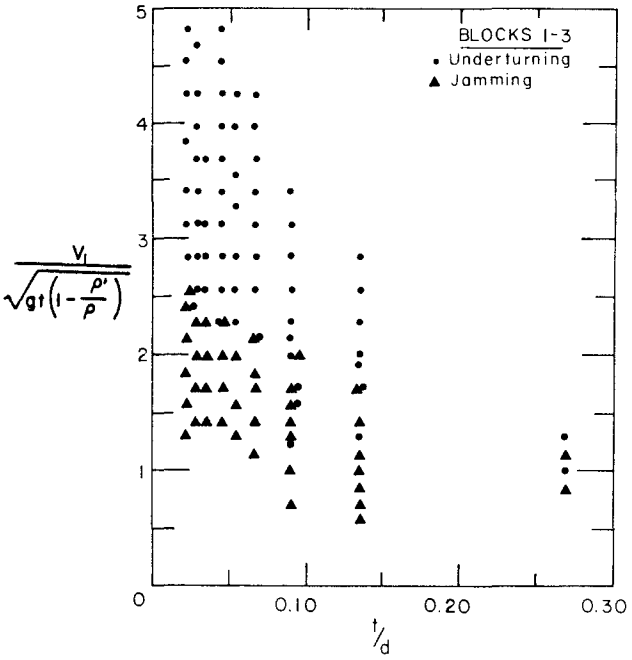

a. Blocks 1-3.

Figure 10 (cont'd).

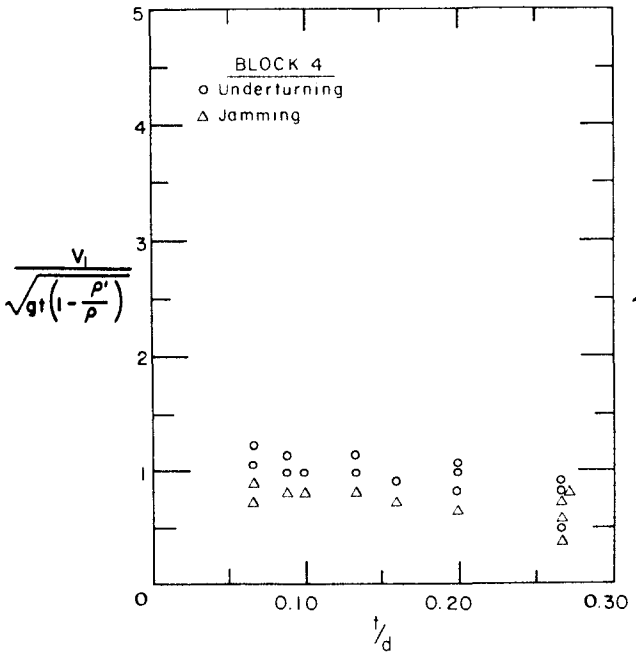

b. Block 4.

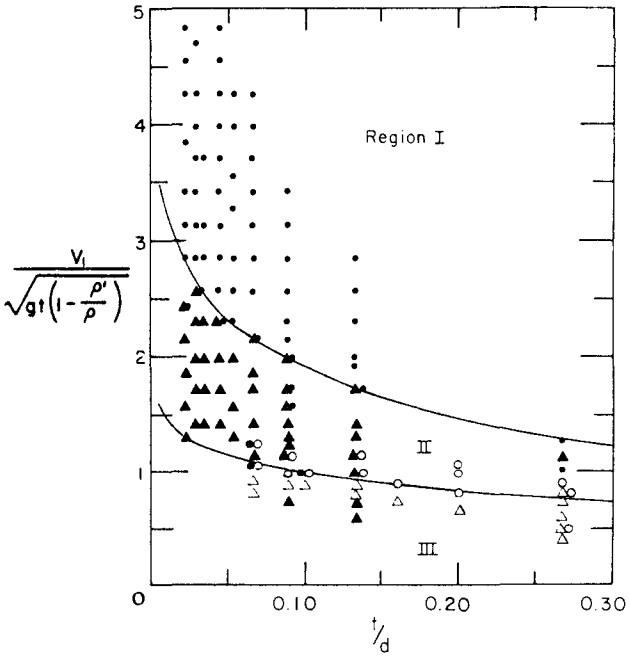

c. All blocks.

Figure 11. Underturning and jamming data.

The velocity of the water was lowered past the underturning region to find the Froude number corresponding to the start of jam formation. In Figure 11a, the jamming data for blocks 1-3 are added to the underturning data for those blocks. Figure 11b shows the similar comparison for block 4. As one would expect, jamming occurs at Froude numbers below the lowest needed for underturning. Figure 11c shows the underturning and jamming points for

all the blocks. There is obviously an area of uncertainty caused by the scatter associated with block thickness. This uncertainty will necessitate basing expectancy on block thickness. In Figure 11c, region I is the area where most ice will pass beneath the bridge; region II is where thicker ice will pass beneath but thinner pieces can be expected to jam; finally, region III is where most blocks will jam against the bridge.

Jamming situations

The consequences of allowing some ice to jam behind the ribbon bridge are unknown since there are no actual data available for the bridge itself. CRREL has done work on the characterization of ice jams and measurement of forces at ice booms, however, that gives us an idea of what to expect in such a situation.

An excellent reference for calculating ice boom loads is EM 1110-2-1612 *Ice Engineering* (Dept. of Army, Corps of Engineers 1982). A brief discussion of the information in this manual follows.

The load on an ice boom comes from the ice cover upstream from it, which is also acted upon by the following:

f_w = shear force from water drag on the underside of the ice
f_a = shear force from wind drag above the ice cover
f_g = weight of the ice because of gravity
f_s = shear force between the ice and shore.

The total force on the boom

$$f_b = f_w + f_a + f_g - f_s.$$

The specific forces are calculated as follows:

$$f_w = \gamma_w S B R_i S$$

where γ_w = specific weight of water (62.4 lb/ft^3)
R_i = hydraulic radius influenced by the ice
S = uniform flow slope
B = channel width.

$$f_a = c \varrho_a u^2 5B$$

where c = a drag coefficient ($1.7 \times 10^{-3} \leq c \leq 2.2 \times 10^{-3}$)
ϱ_a = air density
u = mean wind speed at 30-ft height.

$$f_g = \gamma_i 5BhS$$

where γ_i = specific weight of ice (57.3 lb/ft^3)
h = ice thickness
S = uniform flow slope
B = channel width.

f_s is already factored into the above equations by the term $5B$, the limiting distance from the boom that the above forces interact with the boom. The total force exerted on the boom is then the sum of the above forces. During spring breakup, when there is little resisting force because of friction with the banks, forces of over 300,000 lb have been measured on boom anchor ropes. Perham (1974, 1976, 1977, 1978, 1983) presents more information on ice booms.

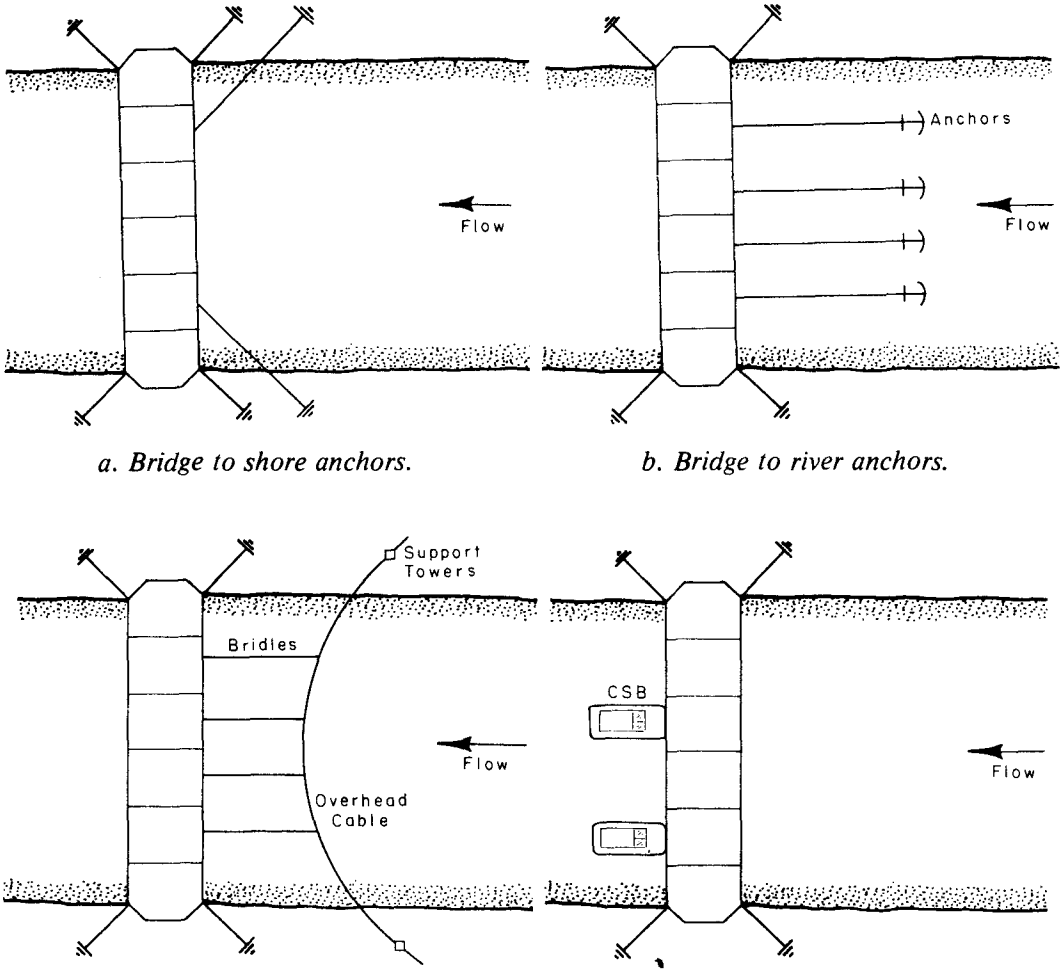

a. Bridge to shore anchors.

b. Bridge to river anchors.

c. Bridge to overhead cable and bridle.

d. Bridge secured with Bridge Erection Boats.

Figure 12. Ribbon Bridge anchoring techniques.

Looking at the bridge shape and means of anchorage, we can determine what reactions to expect in a jamming situation. The bridge is secured in one or a combination of four basic ways:

1. Cables are strung from shore to attach points on the upstream pontons (Fig. 12a).
2. Cables are strung to anchors set upstream of the bridge (Fig. 12b).
3. Cable or rope bridles are dropped from an overhead cable strung across the river (Fig. 12c).
4. Boats are positioned downstream of the bridge to hold it in place (Fig. 12d).

Because they might snag ice or other debris, the anchor system is probably the least desirable. If cables are to be strung from shore, care should be taken to ensure that the catenary clears the water surface to prevent snagging ice and imposing sudden loads on the ponton attach points. The overhead cable and bridle system is the best arrangement for avoiding floating debris. This system would also allow the bridge to "float" upward should ice push beneath it. If there is not a large amount of floating ice and what there is is not unusually large, the Bridge Erection Boat (BEB) can probably be used to secure the bridge. The boat has been shown to be capable of working in an ice environment, within certain limitations, as outlined

by Stubstad et al. (1984). This technique needs further study, however, to ascertain the consequences of floes passing under the bridge and surfacing against the boat.

It is far beyond the scope of this paper to determine forces at every bridge component, but for illustration, a few critical areas are discussed below. The shape of the bow pontons on the ribbon bridge will mitigate the effect of ice accumulating against the bridge since the floes will be deflected downward. The ice will build until 1) the upstream force pushing the ice against the bridge is equalized, 2) the force of buoyancy is exceeded and the ice submerges, or 3) there is a failure in either the connectors, cable anchoring system or bridge structure itself.

The buoyancy force is determined by the size of the ice mass that is exerting the force on the ponton. A 6 by 6 by 1.5 ft piece of ice would need a force of approximately 3370 lb to fully submerge it. Assuming that the 12,000 lb weight of an interior bay is divided evenly between the four pontons that make up a bay, we would have a situation where a bow ponton's weight alone would not be sufficient to submerge the ice. Some of the force of the ice would then be transmitted to an interior roadway ponton via the hinges and ponton bridge latches that hold the bow ponton locked down when the bridge is in the water (Fig. 13). The amount of force taken by this latch is related to the anchoring system being used, the bridge's displacement at the time the ice's force is applied and by what the ice volume is.

We can use as an example the situation of a bay held in place by a BEB. The ice's force can be broken down into horizontal and vertical components applied against the bow ponton (Fig. 14). Each component (F_H and F_v) causes a moment arm about the ponton hinge point which is the product of the force and the distance from the forces' line of application to hinge A (Fig. 15). When the product of $(F_H)(M_H)$ is greater than $(F_v)(M_v)$, there will be a compressive force at the latch. Conversely, when $(F_v)(M_v)$ is greater than $(F_H)(M_H)$, there will be a tensile force on the latch. The point at which the net result of an ice-induced force on the latch is zero is approximately when the bridge is at a displacement equal to zero load or 6-7

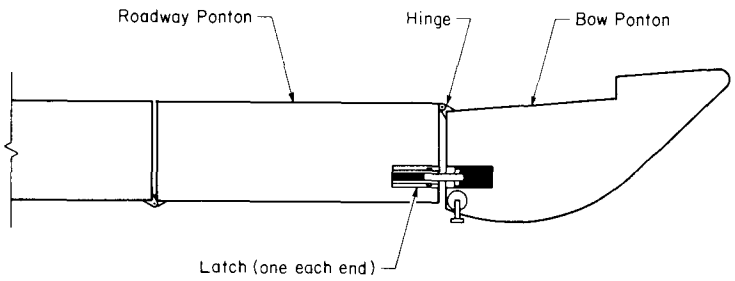

Figure 13. Bow ponton to roadway ponton latch and hinge arrangement.

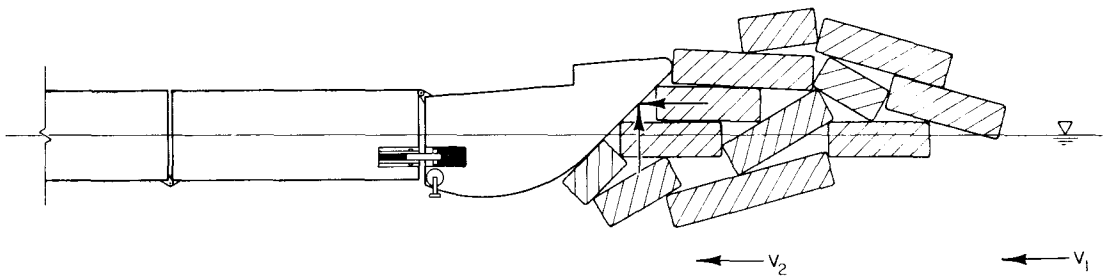

Figure 14. Resolution of forces from jamming ice.

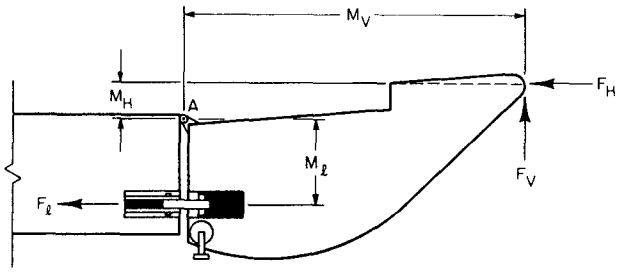

Figure 15. The latch force. F_ℓ *is dependent upon the point of ice force application and the resultant moments about the hinge A.*

in. As the displacement increases, the vertical component of the ice force, F_v, moves further away from the hinge point and $(M_v)(F_v)$ increases. At the maximum expected displacement of 40 in., the moment arm M_v would be approximately 65 in., assuming that the ice force acts at a point on the ponton face where the horizontal component would act through the hinge. The above forces give then 65 in. F_v = 19 in. F_ℓ, where F_ℓ is the force at the latch with a 19-in. moment arm (M_ℓ) from the hinge.

The weight of the ponton acts through its center of gravity, which by a gross calculation is approximately 40 in. from the hinge. The moment due to ponton weight is therefore 3000 lb × 40 in. = 120,000 in. lb. The force due to ice buoyancy upward against the ponton in our example is 3370 lb × 65 in. $(F_v)(M_v)$ = 219,050 in. lb. This leaves an excess of 99,050 in. lb, or roughly 100,000 in. lb of unresolved moment in the vertical direction against the bow ponton. This excess moment must be taken by the latches on either end of the bow pontons. Solving 19 in. $\times F_\ell$ = 100,000 in. lb gives us F_ℓ = 5263 lb for both latches or 5263/2 = 2632 lb for each latch. This force would be in in addition to any force normally on the latch with no load on the bridge, plus any forces imposed by traffic.

The horizontal component of the ice force is offset by the thrust from the BEBs as they hold the bridge in place. These two opposing forces act upon the bridge in opposite directions through the various bridge components. Any bridge bay without a BEB on its downstream face will transmit the ice force via the dogbone connectors to the adjacent bridge bay, which will create a shearing stress in these connectors. Should the adjacent bridge bay have a BEB attached, then a substantial amount of stress can be expected in the connectors between the two bays. The exact magnitude of this stress will depend upon how much horizontal ice force is present and where the next BEB is located.

If the Ribbon Bridge is secured by cables rather than BEBs, the horizontal forces will be taken up by the cable via the attach points at the bridge. The shearing situation would be similar to that described above, with the stress at the dogbone connectors determined by distance between the point where the ice force is applied and the points where cables attach. It is difficult to come up with exact figures for the magnitude of forces involved because of the variety of ways to secure the bridge. If the Ribbon Bridge is to be used in an ice environment, a detailed analysis should be required to asertain if the latches, hinges, dogbone connectors and cable attach points can withstand the additional stress that jamming ice would place upon them. This analysis assumes that the bridge is stationary and does not rebound when it is acted on by the ice. In truth, the forces about the bridge are largely indeterminate and the above is offered only as an illustration.

If, rather than a steady pushing force, the bridge received a sudden impact from a floe carried along with the current, the applied force could be extremely large, depending upon floe size, current velocity, ice density and reaction time of the impact. Impact reaction times are

very difficult to measure and therefore data on impact times from floating ice are practically nonexistent. It should suffice to say that loads on ice boom cables have been measured as high as 300,000 lb because of steady pressure from ice jams, and that impact forces could easily be in this neighborhood.

When an ice jam releases and moves downstream, anything in its path is likely to be destroyed. Bridges should not be deployed when sudden ice movement upstream is likely. If a crossing must be made under these conditions, rafting might be the best alternative. This would minimize equipment and personnel exposure, but must be considered extremely hazardous.

The safest way to conduct a river crossing in ice conditions would be to install an ice boom upstream of the bridging site. CRREL has done several studies on ice booms and their benefits are well documented. Installing a boom provides an ice-free zone to cross in. The procedures would then be similar to summer crossings. There are other problems associated with cold weather river crossings, to be sure, but a channel must be cleared before any crossing can be initiated.

Passing ice

In situations where ice floes will pass beneath the bridge rather than jam against it, there is concern about the impact force of the floes against the upstream face of the bridge and the possibility of damage to protrusions along the bridge surface. As mentioned before, impact forces of individual floes can be substantial and could puncture the bow pontons on the bridge.

Two ways that ice might travel beneath the bridge were discovered during the model tests. In situations where the flow velocity was just above the critical value for instability, the floe would tumble end for end as it pushed beneath the bridge (Fig. 16a). At higher velocities, a floe tended to pass beneath, parallel to the bridge bottom, but would frequently hang up at the back of the downstream ponton (Fig. 16b). Ice striking and accumulating there places a larger force on the downstream ponton latches, with the possiblity of failure. As ice passes through the bridge, one can expect it to build up between pontons and against any protrusions. Eventually, enough ice might be trapped to start a substantial jam, causing uneven pressure under that part of the bridge. This would place stresses on the bar and dogbone connectors and possibly cause some to fail, destroying the integrity of the bridge. Any ice that

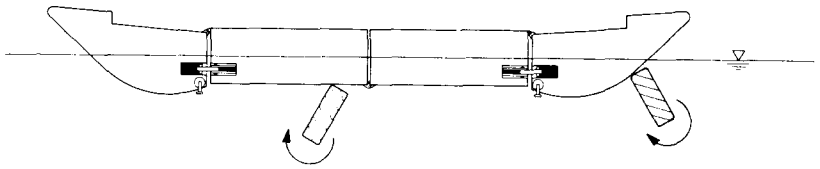

a. Tumbling beneath the bridge.

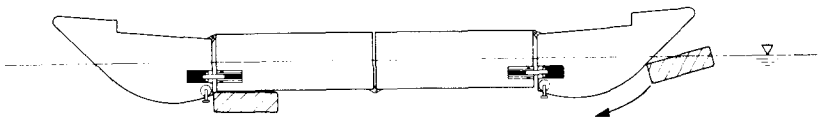

b. "Planar" submergence, passing parallel to bottom bridge surface.

Figure 16. Ice passing modes.

has built up between pontons would impair the retrieval of the bridge sections by hampering the release of the connectors and by preventing individual pontons from folding properly for transport. Problems of this nature were experienced in the winter Reforger exercise of 1985.

CONCLUSIONS AND RECOMMENDATIONS

It has been shown through model studies that there are conditions under which ice can be expected to pass under the Ribbon Bridge and conditions under which ice would jam against it. Both have problems unique to each.

Where ice can pass, impact puncturing is a possibility, along with damage to the bridge by the shearing action of the ice. Retrieval of bridge sections could be difficult with ice packed between the pontons and frozen in connectors.

Jamming situations can place uneven stresses on the bridge sections and anchorages. In these situations traffic should be removed from the bridge to lessen traffic-induced forces on the pontons and latches. The lower displacement that results will cause more ice to pass beneath the bridge, thus lessening total ice accumulation. Excessive ice buildup could snap anchor cables and pull anchors out, while rapid movement of large amounts of ice could easily carry the entire bridge downstream.

A model study alone is not sufficient to detail actual responses of the bridge to icing conditions, but this study provides a general idea of what will happen when the Ribbon Bridge encounters ice.

This study leaves unanswered the questions of retrieval and deployment problems associated with cold weather. It is expected that operation of the bridge hinges and locking mechanisms will be greatly affected by packed snow and ice in various bridge components from both floating ice and the action of vehicles passing over the sections. Rapid retrieval of bridge sections may be impossible when components are frozen.

There are many unknowns in the questions of bridging procedures in cold weather. A comprehensive program needs to be developed to identify specific problems associated with such operations so that there can be a focused approach to solving these problems. The answers obtained from such a program could be invaluable to engineers in the field when they are faced with winter bridging operations.

The theory of block stability has not been well defined for the so-called deep water cases, which in many instances are the situations that arise in practice. The problem has been given a static analysis when it may be more suited to a dynamic energy balance approach. The theory is valuable and is applicable to many practical problems where floating debris is involved. The analysis done in this paper suggests that block thickness plays an important part in the stability equation once the deep water region is entered. The shallow water region seems to be explained well by the present equations based on the block-thickness-to-depth ratio.

LITERATURE CITED

Ashton, G.D. (1974) Froude criterion for ice-block stability. *Journal of Glaciology,* **12**(68): 307–313.

Daly, S.F. (1984) Ice block stability. In *Proceedings, ASCE Hydraulics Division Conference on Water for Resource Development, August 14–17.* New York: American Society of Civil Engineers.

Department of the Army, Corps of Engineers (1982) Ice Engineering. EM 1110-2-1612, 15 October.

Larsen, P. (1975) Notes on the stability of floating ice blocks. In *Proceedings of the Third International Symposium on Ice Problems, 18–21 August, Hanover, New Hampshire.* International Association of Hydraulic Research, pp. 305–314.

Pariset, E. and R. Hausser (1961) Formation and evolution of ice covers on rivers. *Transactions of the Engineering Institute of Canada,* **5**(1): 41–49.

Pariset, E., R. Hausser and A. Gagnon (1966) Formation of ice covers and ice jams in rivers. *Journal of the Hydraulics Division, ASCE,* **92**: 1–24.

Perham, R.E. (1974) Forces generated in ice boom structures. USA Cold Regions Research and Engineering Laboratory, Special Report 200.

Perham, R.E. (1976) Some economic benefits of ice booms. In *Proceedings, 2nd International Symposium on Cold Regions Engineering, August 12–14, Fairbanks, Alaska.* University of Alaska, Cold Regions Engineers Professional Association, pp. 570–591.

Perham, R.E. (1977) St. Marys River ice booms. Design force estimate and field measurement. USA Cold Regions Research and Engineering Laboratory, CRREL Report 77-4.

Perham, R.E. (1978) Performance of the St. Marys River ice booms, 1976-77. USA Cold Regions Research and Engineering Laboratory, CRREL Report 78-24.

Perham, R.E. (1983) Ice sheet retention structures. USA Cold Regions Research and Engineering Laboratory, CRREL Report 83-30.

Uzuner, M.S. and J.F. Kennedy (1972) Stability of floating ice blocks. *Journal of the Hydraulics Division, ASCE,* **98**: 2117–2133.

APPENDIX A: DATA

Water depth (in.)	Water velocity (ft/s)	Block* 1	2	3	4
	Bridge displacement 0.34 in.				
1	0.20	S	S	S	P
	0.26	P	S	S	P
	0.33	P	P	P	P
	0.39	P	P	P	P
	0.46	P	P	P	P
2	0.13	-	-	-	S
	0.16	-	-	-	P
	0.20	-	-	-	P
	0.26	S	S	S	P
	0.33	P	P	S	P
	0.39	P	P	S	P
	0.49	P	P	P	P
	0.59	P	P	P	P
3	0.16	S	S	S	P
	0.23	S	S	S	P
	0.33	P	S	S	P
	0.39	P	P	S	P
	0.46	P	P	S	P
	0.53	P	P	P	P
	0.62	P	P	P	P
	Bridge displacement 1.5 in.				
2	0.23	S	S	S	S
	0.33	S	S	S	P
	0.39	U	U	S	P
	0.46	U	U	U	P
	0.53	U	U	U	P
	0.59	P	P	U	P
	0.66	P	P	U	P
	0.72	P	P	P	P
3	0.30	S	S	S	S
	0.33	S	S	S	U
	0.36	S	S	S	P
	0.39	U	U	S	P
	0.46	U	U	U	P
	0.59	U	U	U	P
	0.66	U	U	U	P
	0.72	U	U	P	P
	0.79	U	P	P	P
	0.85	P	P	P	P
	0.92	P	P	P	P
5	0.30	S	S	S	S
	0.36	S	S	S	U
	0.46	S	S	S	P
	0.53	U	U	U	P
	0.59	U	U	U	P
	0.66	U	U	U	P
	0.75	P	U	U	P
	0.82	U	U	P	P
	0.92	P	U	P	U
	0.98	U	P	P	P
	1.05	P	P	P	P
8	0.33	S	S	S	S
	0.39	S	S	S	U
	0.46	S	S	S	P
	0.53	S	S	S	P
	0.59	U	U	U	P
	0.66	U	U	U	P
	0.72	U	U	U	P
	0.79	P	P	P	P
	0.85	U	U	P	P
	0.92	P	P	P	P
	0.98	P	P	P	P
	Bridge displacement 2 in.				
3	0.23	S	S	S	S
	0.30	S	S	S	S
	0.33	S	S	S	S
	0.39	S	S	S	P
	0.46	S	U	U	P
	0.53	U	U	U	P
	0.59	U	U	U	P
	0.66	U	U	U	P
	0.72	U	U	P	P
	0.79	P	P	P	P
4	0.26	S	S	S	S
	0.33	S	S	S	S
	0.39	S	S	S	U
	0.43	S	S	S	U
	0.49	S	U	U	P
	0.59	U	U	U	P
	0.66	U	U	U	P
	0.72	U	U	U	P
	0.79	U	U	U	P
	0.85	U	U	U	P
	0.92	U	U	P	P
	0.98	P	U	P	P

Water depth (in.)	Water velocity (ft/s)	Block*			
		1	2	3	4
6	0.33	S	S	S	S
	0.39	S	S	S	U
	0.46	S	S	S	U
	0.53	S	S	U	P
	0.59	U	U	U	P
	0.66	U	U	U	P
	0.72	U	U	U	P
	0.79	U	U	U	P
	0.85	U	U	U	P
	0.92	P	U	U	P
	0.98	U	U	P	P
	1.05	U	U	P	P
	1.12	U	U	P	P
9	0.33	S	S	S	S
	0.39	S	S	S	U
	0.46	S	S	S	U
	0.53	S	S	S	P
	0.59	S	S	U	P
	0.66	U	U	U	P
	0.72	U	U	U	P
	0.79	U	U	U	P
	0.85	U	U	U	P
	0.92	U	U	U	P
	0.98	U	U	U	P
	1.08	U	U	P	P
	1.15	P	P	P	P
12	0.30	S	S	S	S
	0.36	S	S	S	S
	0.43	S	S	S	U
	0.49	S	S	S	U
	0.56	S	S	U	P
	0.66	U	U	U	P
	0.72	U	U	U	P
	0.79	U	U	U	P
	0.89	U	U	U	P
	0.98	U	U	P	P
	1.05	U	U	P	P
	1.12	U	P	P	P

*S - stable; U - underturning and tumbling;
P - planar passing